The Effect of The Contaminant Source and Air Outlet Locations on The Performance of The Environmental Displacement Ventilation System

Dr. Alsayed A. El-Agouz
Mech. Engineering. Dept.
Faculty of Engineering., Tanta
Tanta University

Dr. Essaied M. Shuia
Mech. Engineering. Dept.
Faculty of Engineering., Zawia
Zawia University

Abstract:

This paper presents an investigation of the effect of the contaminant source and air outlet locations on the performance of the environmental displacement ventilation system using a numerical simulation. Laminar steady mixed convection in a two-dimensional displacement ventilated room with discrete heat and contaminant sources is studied. The solution is determined by Grashof and Reynolds numbers and their influence on the resulting thermal comfort and indoor air quality. The discussed thermal comfort parameters include temperature distribution and ventilation effectiveness for the heat removal. The indoor air

quality is determined by investigating the contaminant distribution, ventilation effectiveness for contaminant removal, and air cleaning efficiency.

It is found that the Reynolds number is more than 300, The locations of the contaminant source and air outlet have no major influence on the heat transfer rate and the heat removal effectiveness ε_h and the air clearing efficiency ξ while the mass transfer rate and the contaminant removal effectiveness are influenced. The heat and mass transfer rates, the heat and contaminant removal effectiveness and the air clearing efficiency are more influenced by the locations of the contaminant source and air outlet for Reynolds number less than 300. Results for different outlet locations show that the closer the outlet is to the heat and contaminant sources, the more effective is to vent heat and contaminant generated by the sources.

Keywords:

CFD; Mixed convection; Displacement ventilation; Discrete heat/Contaminant sources

Nomenclature:

Br	buoyancy ratio
c, C	dimension and dimensionless concentrations
D	mass diffusivity
g	gravity acceleration
Gr	Grashof number
h	sizes of inlet or outlet
k	thermal conductivity (W/m. K)
L	length or length of the room
Nu_m	average Nusselt number
p, P	dimension and dimensionless pressures
Pr	Prandtl number
Ra	Rayleigh number
Re	Reynolds number
Sc	Schmidt number
Sh_m	average Sherwood number
t	temperature
U, V	dimensionless velocities in X and Y directions

u, v	velocity components in x and y directions
x, y	Cartesian coordinates
X, Y	dimensionless Cartesian coordinates

Greek symbols:

β	thermal expansion coefficient
ρ	density
ε_h	ventilation effectiveness for the heat
ε_c	ventilation effectiveness for contaminant
α	thermal diffusivity
ν	kinematic viscosity
ϕ	general variable
ω	dimensionless vorticity
θ	dimensionless temperature
Ψ	dimensionless stream function
μ	contamination degree
ε	aspect ratio
ξ	air cleaning efficiency

Subscripts:

c	concentration
cs	contaminant source
h	high
hs	heat source
i	local
in	inlet
m	mean
out	outlet
t	thermal

1. Introduction:

Ventilation systems in buildings should be designed for the health and comfort of the occupants. One of the main aims is to create an acceptable thermal environment without draught problems. Draught is defined as unwanted local cooling of the human body caused by air movement. The draught sensation increases when the air temperature decreases and the air velocity increases. Indoor air quality and thermal comfort are the most important characteristics of an indoor environment. As people spend more time indoors, heating, ventilating and air-conditioning systems that provide high indoor air quality and thermal comfort, become very important. In room air distribution, there are usually two methods of supplying the air: either mixing ventilation or displacement ventilation. In mixing ventilation, air is normally supplied at high level over the ceiling which is then deflected down into the occupied zone by the opposite walls thus causing a mixing of the air jet with room air. In displacement ventilation, the air is supplied at low level, usually over the floor, and then rises up due to buoyancy before it is extracted at high level. In displacement ventilation, both natural and forced convection must be taken into account. The interaction between the two convective flows is important to achieve the effectiveness of ventilation. Visualizing the processes may provide a new means to understand the philosophy.

Gan [4 and 5] used computational fluid dynamics to study air distribution systems in the room and used computational fluid dynamics (CFD) to investigate local thermal discomfort in an office room. Also, Nielsen [13] analyzed the velocity distribution in a room ventilated by displacement ventilation and wall-mounted air terminal devices. Xing et. al.[9] presented a study of the air quality in the breathing zone in a room with displacement ventilation.

Chen et al. [14] presented the field distributions of air velocity, temperature, contaminant concentration, and thermal comfort in an office with displacement ventilation for different air supply parameters such as the effective area, shape, dimension of the diffuser, the turbulence intensity, flow rate, and temperature of the air supplied. The analysis indicated that, the effects of the effective area, shape, dimension of the diffuser and the turbulence intensity of the air supplied have little effect on the room air diffusion except at floor level. In addition, the influence of the flow rate and temperature of the air supplied is very significant on the air diffusion as well as on the thermal comfort and indoor air quality.

Wyon and Sandberg [3] performed a series of experiments on the thermal comfort of the displacement ventilation system using a manikin. They found that the thermal comfort was better above table height and thermal discomfort was mostly observed at the legs and ankles. Lian [20] investigated the upward displacement ventilation system to determine the effect of the type of outlet, distance between the occupant and outlet, velocity and temperature of supply air, and the type of outlet. The results show that the main influence on the thermal comfort is the distance between the occupant and the supply.

Awbi [6] compared the effectiveness of mixing and displacement ventilation in terms of heat and contaminant removal. Results were presented for CFD simulations of the air movement in the chamber and for measurements using a heated manikin with displacement ventilation. The CFD simulations and the measurements suggest that displacement ventilation was more energy efficient than a mixing system.

The effects of a primary convective heat gain as the vertical location of the source changes on displacement ventilation systems were investigated numerically by Park and Holland [10]. The study suggested that, when the heat source raised, the temperature field changed, the convective heat gain from the heat source to an occupied zone becomes less significant and the cooling load decreased in that region. In addition, the stratification level is also affected by the heat source location at a given flow rate.

Deng and Tang [15] investigated the mixed convection, two-dimensional, steady and laminar displacement ventilation model. The analysis was based on the fluid flow and heat transfer characteristics of the displacement ventilation using the method of streamlines and heat lines. The analysis was performed for Grashof number in the range of 10^3–10^6. The results and comparisons showed that the displacement ventilation guarantees a high indoor air quality (IAQ) and was therefore a desired air-conditioning system.

Laminar double diffusive mixed convection in a two-dimensional displacement ventilated enclosure with discrete heat and contaminant sources was studied numerically by Deng et al. [16]. The study was aimed at evaluating the influence of the strength of heat source, the strength of contaminant source, the strength of ventilation and the ventilation mode on the indoor air environment. They indicated that the convection transport method could explicitly disclose the complicated philosophy of indoor air environment, and thus provides a simple but

practical approach to see the indoor airflow and heat and contaminant transport structures.

Lin et al. [21] studied numerically the effect of the air supply location on the design and performance of the displacement ventilation system. The results reported in terms of thermal comfort and indoor air quality. The results indicated that the supply should be located near the centre of the room rather than to one side of the room. In addition, the exhaust was found to have minimal effect on the thermal comfort.

Kosonen [17] studied the effect of supply air systems on the efficiency of a ventilate ceiling. The author found that using the ceiling supply and capture jet concept, the contaminant removal efficiency was reached to 85% by increasing the airflow rate 20% compared with the theoretical plume equation.

The objective of this paper is to analyze the effect of the contaminant source and air outlet locations on the performance of the environmental displacement ventilation system. Laminar, steady, and mixed convection in a two-dimensional displacement ventilated room with discrete heat and contaminant sources is numerically studied. Efforts are concentrated on the effects of Reynolds number, Grashof number and the ventilation mode on the room environmental displacement ventilation characteristics. Mixed convection has been studied for Reynolds number varied from 50 to 600 and Grashof number from 10^4 to 1.5×10^8. This paper focuses on both thermal comfort and indoor air quality. The thermal comfort parameters include temperature distribution and ventilation effectiveness for heat removal (ε_t). The indoor air quality is determined by investigating the contaminant distribution, ventilation effectiveness for the contaminant removal (ε_c), and the air cleaning efficiency (ξ).

2. Physical model:

The physical model of displacement ventilation under consideration is considered here and is schematically shown in Fig. (1a). It is a two-dimensional ventilated square room, with sides of length L. A heat source of size L_{hs} and high temperature t_h, located at the center of the floor wall, and a contaminant source of size L_{cs} and high concentration c_h located at the center of the right wall. The fresh cold air (u_{in}, t_{in}, c_{in}) is supplied from the inlet at the bottom of left side wall and the polluted hot air exhausted from the top of right side wall. The inlet and outlet are of the same size, h. Other parts of the room are all considered adiabatic. The

different locations of the contaminant source and air outlets are shown in Fig. (1b, 1c, 1d. 1e, 1f).

3. Governing equations:

The analysis based on the two-dimensional steady continuity, momentum, and energy equations in dimensionless form.

1) The flow is steady, incompressible, and laminar.
2) The air and the contaminant gases are perfectly mixed.
3) All the thermo-physical of the fluid properties is constant, except that the density in the buoyancy term of the momentum equation following the Boussinesq approximation.

Considering the above assumptions, the governing equations of continuity, momentum, energy and concentration equations can be written in a non-dimensional form, as follows:

Continuity equation

$$\frac{\partial U}{\partial X}+\frac{\partial V}{\partial Y}=0 \qquad (1)$$

Momentum equations

$$\left[U\frac{\partial U}{\partial X}+V\frac{\partial U}{\partial Y}\right]=-\left(\frac{\partial P}{\partial X}\right)+\frac{1}{\mathrm{Re}}\left[\frac{\partial^2 U}{\partial X^2}+\frac{\partial^2 U}{\partial Y^2}\right] \qquad (2)$$

$$\left[U\frac{\partial V}{\partial X}+V\frac{\partial V}{\partial Y}\right]=-\left(\frac{\partial P}{\partial Y}\right)+\frac{1}{\mathrm{Re}}\left[\frac{\partial^2 V}{\partial X^2}+\frac{\partial^2 V}{\partial Y^2}\right]+\frac{Gr}{\mathrm{Re}^2}(\theta+Br\,C) \qquad (3)$$

Energy equation

$$\left[U\frac{\partial \theta}{\partial X}+V\frac{\partial \theta}{\partial Y}\right]=\frac{1}{\mathrm{Re}\,\mathrm{Pr}}\left[\frac{\partial^2 \theta}{\partial X^2}+\frac{\partial^2 \theta}{\partial Y^2}\right] \qquad (4)$$

Concentration equation

$$\left[U\frac{\partial C}{\partial X}+V\frac{\partial C}{\partial Y}\right]=\frac{1}{\mathrm{Re}\,Sc}\left[\frac{\partial^2 C}{\partial X^2}+\frac{\partial^2 C}{\partial Y^2}\right] \qquad (5)$$

The governing equations are non-dimensionalized using scales L, u_{in}, $\Delta t=(t_h-t_{in})$, and $\Delta c=(c_h-c_{in})$ for length, velocity, temperature, and concentration respectively. Accordingly the dimensionless variables are $(X,Y)=(x,y)/L$, $(U,V)=(u,v)/u_{in}$, $P=p/\rho u_{in}^2$, $\theta=(t-t_{in})/\Delta t$, $C=(c-c_{in})/\Delta c$ and

dimensionless parameters are defined as $Pr = \upsilon / \alpha$, $Gr = g\beta_t \Delta t L^3 / \upsilon^2$, $Re=u_{in}L/\upsilon$, $Sc=\upsilon/D$, $Br=\beta_c \Delta c/\beta_t \Delta t$

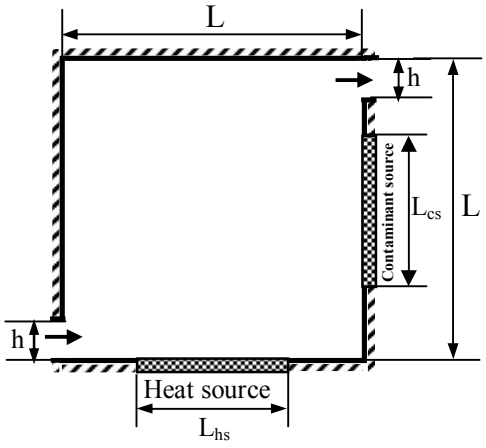

(a)

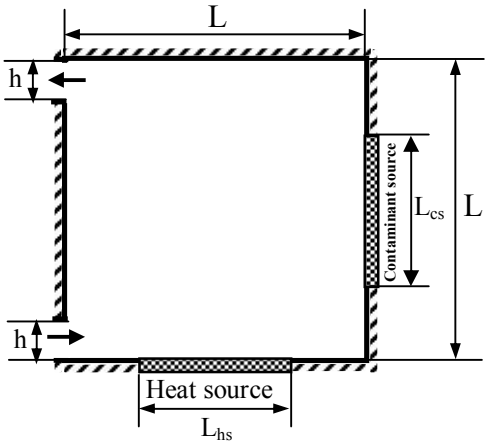

(d)

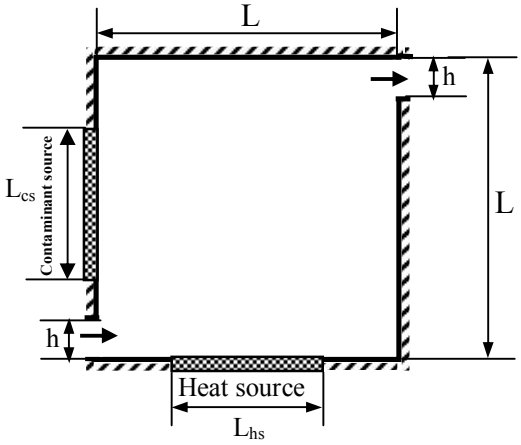

(b)

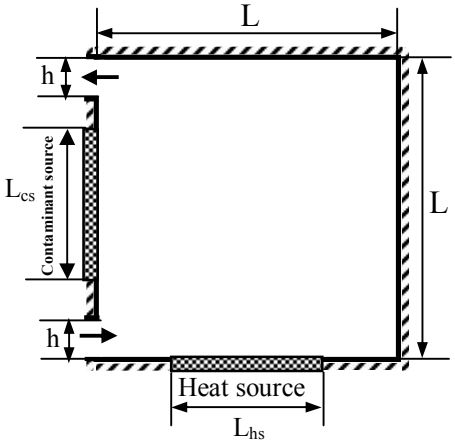

(e)

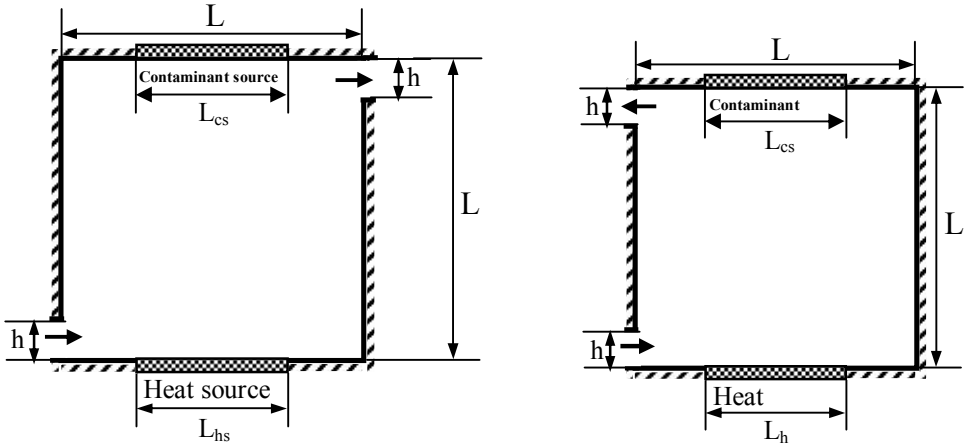

(c) (Case 1) (f) (Case 2)

Fig. 1 Schematic diagram of physical configuration cases considered in the study

In the following analysis, the vorticity-stream function formulation is introduced in the mathematical model. In order to satisfy the continuity equation, the dimensionless vorticity-stream function is defined as $U=\partial\psi/\partial Y$, $V=-\partial\psi/\partial X$ and

$-\omega=(\partial^2\psi/\partial X^2+\partial^2\psi/\partial Y^2)$.

In terms of the above definitions, the dimensionless form of the momentum equation can be expressed as follows:

$$\left[U\frac{\partial\omega}{\partial X}+V\frac{\partial\omega}{\partial Y}\right]=\frac{1}{\mathrm{Re}}\left[\frac{\partial^2\omega}{\partial X^2}+\frac{\partial^2\omega}{\partial Y^2}\right]+\frac{Gr}{\mathrm{Re}^2}\left[\frac{\partial\theta}{\partial X}+Br\frac{\partial C}{\partial X}\right] \qquad (6)$$

The model of the governing equations is represented in function of the dimensionless velocities (U, V), concentration (C), temperature (θ), vorticity (ω) and the stream function (ψ).

The average Nusselt and Sherwood numbers describe the heat and mass transfer rates on the surfaces of heat and contaminant sources are expressed as follows:

$$Nu_m=\frac{1}{\varepsilon_{hs}}\int_{(1-\varepsilon_{hs})/2}^{(1+\varepsilon_{hs})/2}-(\partial\theta/\partial n).dX \qquad (7)$$

$$Sh_m=\frac{1}{\varepsilon_{cs}}\int_{(1-\varepsilon_{cs})/2}^{(1+\varepsilon_{cs})/2}-(\partial C/\partial n).dX \qquad (8)$$

ε_{hs} and ε_{cs} are set equal to 0.5 for the study

4. Ventilation parameters:

The purpose of ventilation is the provision of uncontaminated air and the removal of internally produced contaminants from the building. Very often the process also involves the distribution of heating or cooling in the building. It is, therefore, a process which involves both diffusion and convection heat. The pattern of air flows in the room being ventilated will largely determine the diffusion and convection processes. This is influenced by the air supply and room characteristics. Such characteristics will involve air jet velocity, temperature difference between the air jet and room air, position and type of air supply device, distribution of room heat and contaminant sources, etc. There are many parameters which can be quantified by measurement or CFD simulation which can be used to assess the effectiveness of the ventilation system.

4.1. Ventilation effectiveness for heat removal (ε_h)

The ventilation effectiveness for heat removal reflects the ability of the ventilation system to remove heat and it is defined by:

$$\varepsilon_h = \frac{\theta_{out} - \theta_{in}}{\theta_m - \theta_{in}} \qquad (9)$$

4.2. Ventilation effectiveness for contaminant removal (ε_c)

This is a measure of how effective the ventilation system is in removing internally produced contamination. It is defined by:

$$\varepsilon_c = \frac{C_{out} - C_{in}}{C_m - C_{in}} \qquad (10)$$

where θ_{in} and C_{in} are the dimensionless temperature and contaminant concentration of inlet air, (typically zero), respectively; θ_{out} and C_{out} are the dimensionless temperature and contaminant concentration of outlet air, respectively; θ_m and C_m are the mean values for dimensionless temperature and contaminant concentration of air in the occupied zone, respectively. The occupied zone is defined as the space from floor to 1.8 m high and 0.15 m away from side walls.

The parameters, θ_m and C_m calculated from *N* measured locations. If the measured points were uniformly spaced within the room volume, the mean dimensionless temperature and contaminant concentration is simply given by:

$$\theta_m = \frac{1}{N}\sum_{i=1}^{N}\theta_i \qquad C_m = \frac{1}{N}\sum_{i=1}^{N}C_i$$

where θ_i and C_i are the local dimensionless temperature and contaminant concentration, respectively

4.3. Air cleaning efficiency (ξ)

ASHRAE [1] recommends using the air cleaning efficiency, ξ, to evaluate such configurations, where ξ is calculated from:

$$\xi = 1 - C_{out} \qquad (12)$$

5. Boundary conditions:

The boundary conditions of the above governing equations, for the considered problem, are as:

Inlet: $U=1$, $V=0$, $\theta=0$ and $C=0$;

Outlet: $\partial U/\partial n = 0$ and $\partial\theta/\partial n = 0$, $\partial C/\partial n = 0$

Walls: $U=V=0$, $\theta=1$ for the heat source and $\partial\theta/\partial n = 0$ elsewhere, $C=1$ for contaminant source and $\partial C/\partial n = 0$ elsewhere.

6. Numerical procedure:

A finite volume procedure discussed by Patanker [18] and Versteeg and Malalasekera [7] was used to solve the dimensionless governing equations and the associated boundary conditions. To simplify the numerical solution, the governing equations for the variables θ, ψ, C and ω can be formulated as a diffusion-convection equation as follows:

$$\frac{\partial}{\partial X}(\beta\Phi U) + \frac{\partial}{\partial Y}(\beta\Phi V) = \frac{\partial}{\partial X}(\Gamma\frac{\partial\Phi}{\partial X}) + \frac{\partial}{\partial Y}(\Gamma\frac{\partial\Phi}{\partial Y}) + (S_u + S_p\Phi) \qquad (13)$$

The two terms in the left-hand side of Eq. (13), are the convective terms, while the first and second terms of the right-hand side represent the diffusion terms, the third is the source term, Φ represents any one of the variables (Φ=ψ, ω, C and θ), and Γ is the diffusion coefficient.

The integration of the diffusion-convection equation (13) over the control volume and the terms have been discredited using the upwind scheme to the convective terms while central differencing scheme to diffusion and source terms. Then, the discretized equation (13) has the following form:

$$\Phi_P = (a_E\Phi_E + a_W\Phi_W + a_N\Phi_N + a_S\Phi_S + b)/a_P \qquad (14)$$

Where:

$$a_E = \frac{\Gamma}{\Delta X^2} - \beta\left[\frac{U_e - |U_e|}{2\Delta X}\right]; a_W = \frac{\Gamma}{\Delta X^2} + \beta\left[\frac{U_w - |U_w|}{2\Delta X}\right]; a_N = \frac{\Gamma}{\Delta Y^2} - \beta\left[\frac{V_n - |V_n|}{2\Delta Y}\right]$$

$$a_S = \frac{\Gamma}{\Delta Y^2} + \beta\left[\frac{V_s - |V_s|}{2\Delta Y}\right]; \Delta f = \beta\left[\frac{U_e - U_w}{\Delta X} + \frac{V_n - V_s}{\Delta Y}\right],$$

$$a_P = (a_E + a_W + a_N + a_S + \Delta f - \bar{S}_P); \quad b = \bar{S}_u$$

Applying the above discretization procedure, the values of Γ, β, and b for the governing equations of the variables ψ, ω, C and θ are given in Table 1.

The obtained algebraic equations of the dimensionless governing equations were solved using the Gauss-elimination method. An iterative solution procedure was employed to obtain the steady state solution of the considered problem. The convergence criteria was used for all field variables for every point is:

$$\left|(\phi_{m+1} - \phi_m)/\phi_m\right|_{\max} \le 10^{-6},$$

Where: m is the index representing the number of iterations.

In order to ensure the grid-independence solutions, a series of trial calculation were conducted for different grid distributions: 40×40, 65×65, 81×81, and 97×97. Table 2 presents a comparison of the predicted average Nusselt numbers and average Sherwood number, using different grid arrangements, for the case of Re = 500, Sc=Pr=0.7 and Gr=10^6. It was observed that there is a difference between the result of the grid 81×81 and that of the grid 97×97 is less than 0.342% and 0.016% for average Nusselt numbers and average Sherwood number. Consequently, to optimize appropriate grid refinement with computational efficiency, the grid 97×97 was chosen for all the further computations.

Table 1 Values of Γ, β, and b for the variables C, θ, ψ and ω

Φ	C	θ	ψ	ω
β	1	1	0	1
Γ	1/Re Sc	1/Re Pr	1	1/Re
b	0	0	ω_P	$Gr/Re^2[(\theta_E - \theta_W) + Br(C_E - C_W)]$

Table 2: The comparison of the predicted average Nusselt and Sherwood numbers at different grid distribution for the case of Re = 500, Sc=Pr=0.7 and Gr=10^6.

Grid	40×40	65×65	81×81	97×97
$\overline{Nu}$	13.82614	14.62265	14.75633	14.80682
$\overline{Sh}$	8.338936	8.351422	8.353457	8.354799

7. Model validation:

The accuracy of the numerical model was verified by comparing the results from the present work with the corresponding numerical results reported by Calcagni et al. [2]. The model studied free convective heat transfer in a square enclosure characterized by a discrete heater located on the lower wall and cooled from the lateral walls. The commercial finite volumes code Fluent 6.0 was used in analysis.

The comparison between the present work and numerical results reported by Calcagni et al. [1] is shown in Fig. 2. Fig. 2 presents the numerical temperature contours at ε_{hs} = 4/5 for Ra = 10^3, 10^4, and 10^5. The results of the present model have a good overall agreement with Calcagni numerical results.

8. Results and discussions:

In the present study, the aspect ratios of the ventilated room, the heat source, the contaminant source, the inlet air and outlet air of what are kept constant as ε_r =1, ε_{hs} = ε_{cs}=0.5, ε_{in} =ε_{out} =1/8. The buoyancy ratio, Prandtl and Schmidt numbers are held fixed at Br=10, Pr =Sc = 0.7. The effect of the contaminant source and air outlet locations on the performance of the environmental displacement ventilation is studied. During the study the Rayleigh number is varied from 10^4 to 1.5×10^8 and Reynolds number is varied from 50 to 600.

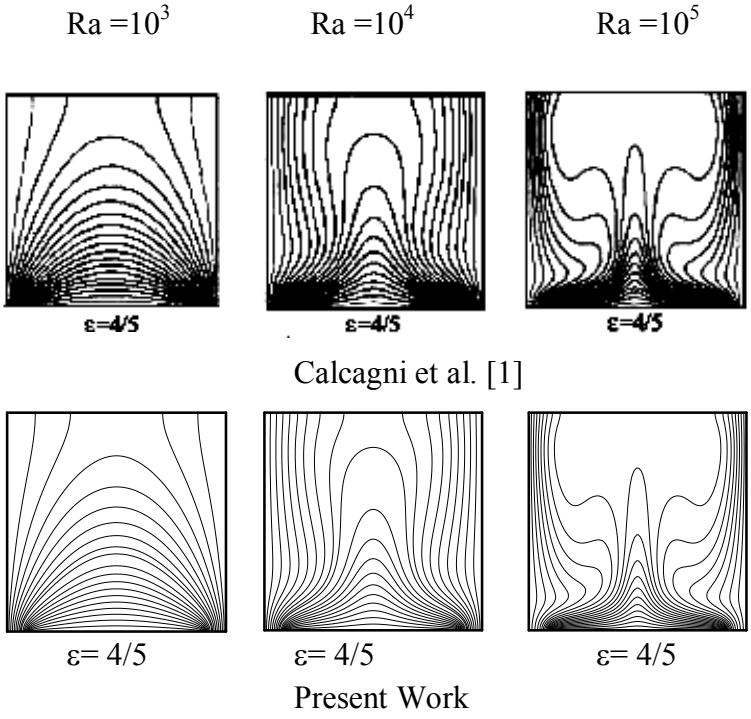

Fig. 2 Comparison between the present work and Calcagni et al. [1] for numerical temperature contours at ε = 4/5 for Ra = 10^3, 10^4, and 10^5

8.1 The thermal comfort:

Figure 3 shows the isotherm contours with Re at different Gr levels. With the increase of the Grashof and Reynolds numbers, the buoyancy forced generated by the heat source and the external forced cold flow is strong enough to dominate the flow structure. Therefore, the isotherm contours decrease with the increase of the Grashof and Reynolds numbers. The θ_m of air in the occupied zone for the case 1 is better than that in case 2. This is due to the fact that longer transport path of the right outlet air than the left outlet air. For $\mathrm{Re} \rangle 300$, the mean values for dimensionless temperature of air in the occupied zone for the case 1 and case 2 are less effected by increasing the Gr and Re.

Figure 4 shows the variation of the average Nusselt number as a function of Reynolds number, Re, at different Grashof numbers for cases 1 and 2. It is observed that, for $10^4 \langle \mathrm{Gr} \langle 10^7$, the average Nusselt number increases with increasing the Reynolds number. At $\mathrm{Gr} = 10^8$ and 1.5×10^8, $\mathrm{Nu_m}$ decreases slowly with the increase of Re, then reaches a minimum value at $\mathrm{Re} = 100$, beyond

which increases with the increasing Re. Beyond that point, $\mathrm{Re} \rangle 300$, the average Nusselt number has small effect with the Gr increase. At $\mathrm{Re} \equiv 600$, the average Nusselt number at the right outlet air (case 1) was about 16.4 compared to about 15.7 for the left outlet air (case 2). It is observed that, there is little difference in the average Nusselt number due to the locations of the contaminant source and air outlet.

Figure 5 shows the effect of Reynolds number on the heat removal effectiveness, ε_h, for different Grashof numbers. The ventilation effectiveness for heat removal decreases with the increase of Reynolds number. For $\mathrm{Re} \langle 300$, the ventilation effectiveness is influenced by increasing the Gr and is also affected by the location of the outlet air due to the cooperation between the natural and forced convection is gradually enhanced. Beyond that point, $\mathrm{Re} \rangle 300$, the ventilation effectiveness is less effected by increase the Gr and Re. At $\mathrm{Re} = 600$, the ventilation effectiveness at the right outlet air (case 1) was about 0.207 compared to about 0.234 for the left outlet air (case 2). This is due to dominate the airflow by the forced convection. This means that the locations of the contaminant source and outlet air have no major influence on the ventilation effectiveness. The ventilation effectiveness at the occupied zone is small because the heat source lies farther from exhaust, and thus a longer transport path is required for heat removal, as indicated by the isothermal line.

8.2 The indoor air quality:

Figure 6 shows the evolution of contaminant contours for different Re and Gr levels for cases 1 and 2. With the increase of the Grashof and Reynolds numbers, the contaminant contours decreases. For the contaminant source at right, C_m of air in the occupied zone for the case 1 is better than that in case 2. On the other hand, for the contaminant source at left, C_m of air in the occupied zone for the case 2 is better than that in case 1. This is due to nearer location of the contaminant source from the location of the outlet air. For the contaminant source at top, C_m of air in the occupied zone for the cases 1and 2 is less affected by the locations of the outlet air.

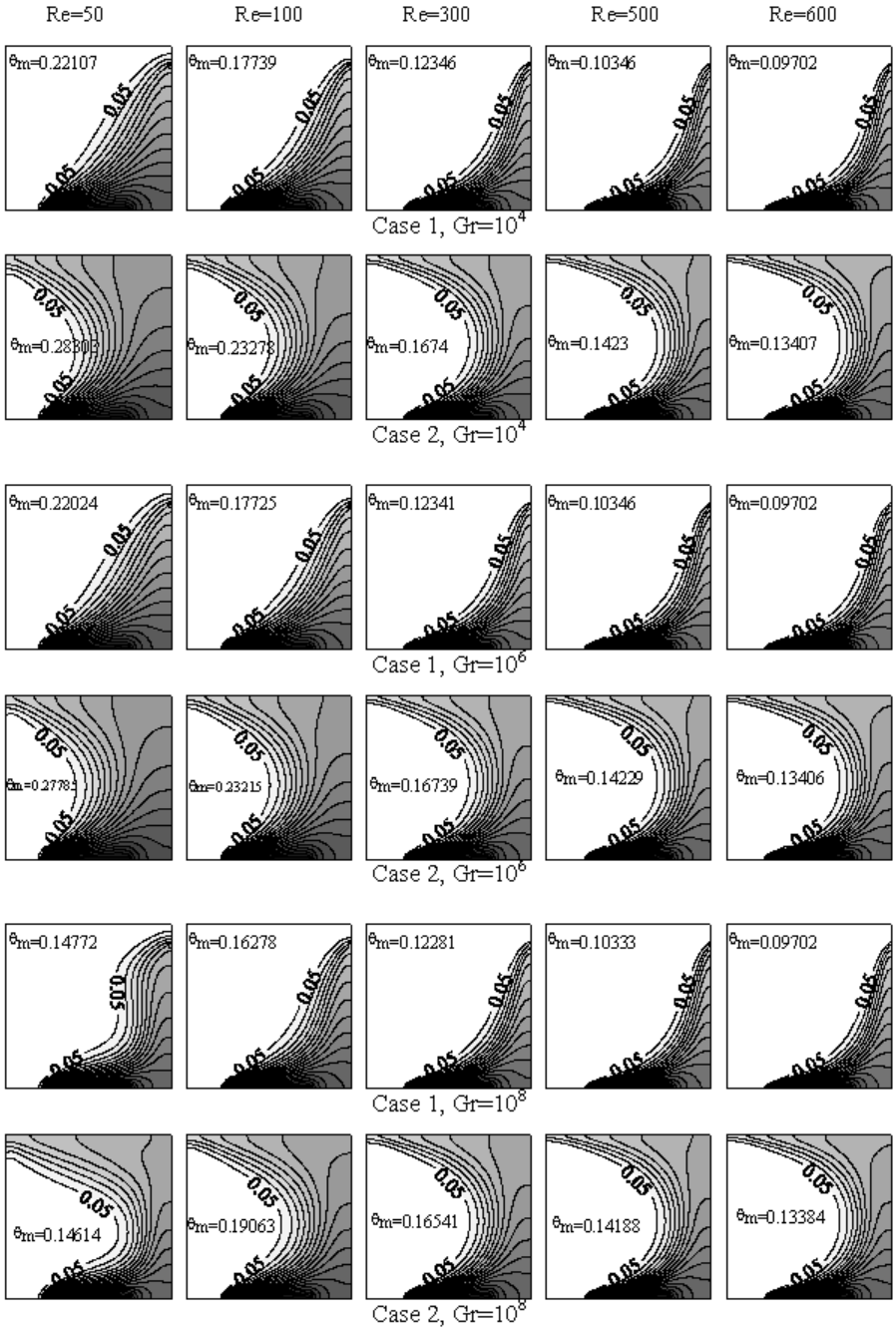

Fig. 3 Isotherm contours for different Re & Gr numbers and dimensionless mean temperature for case 1 and case 2

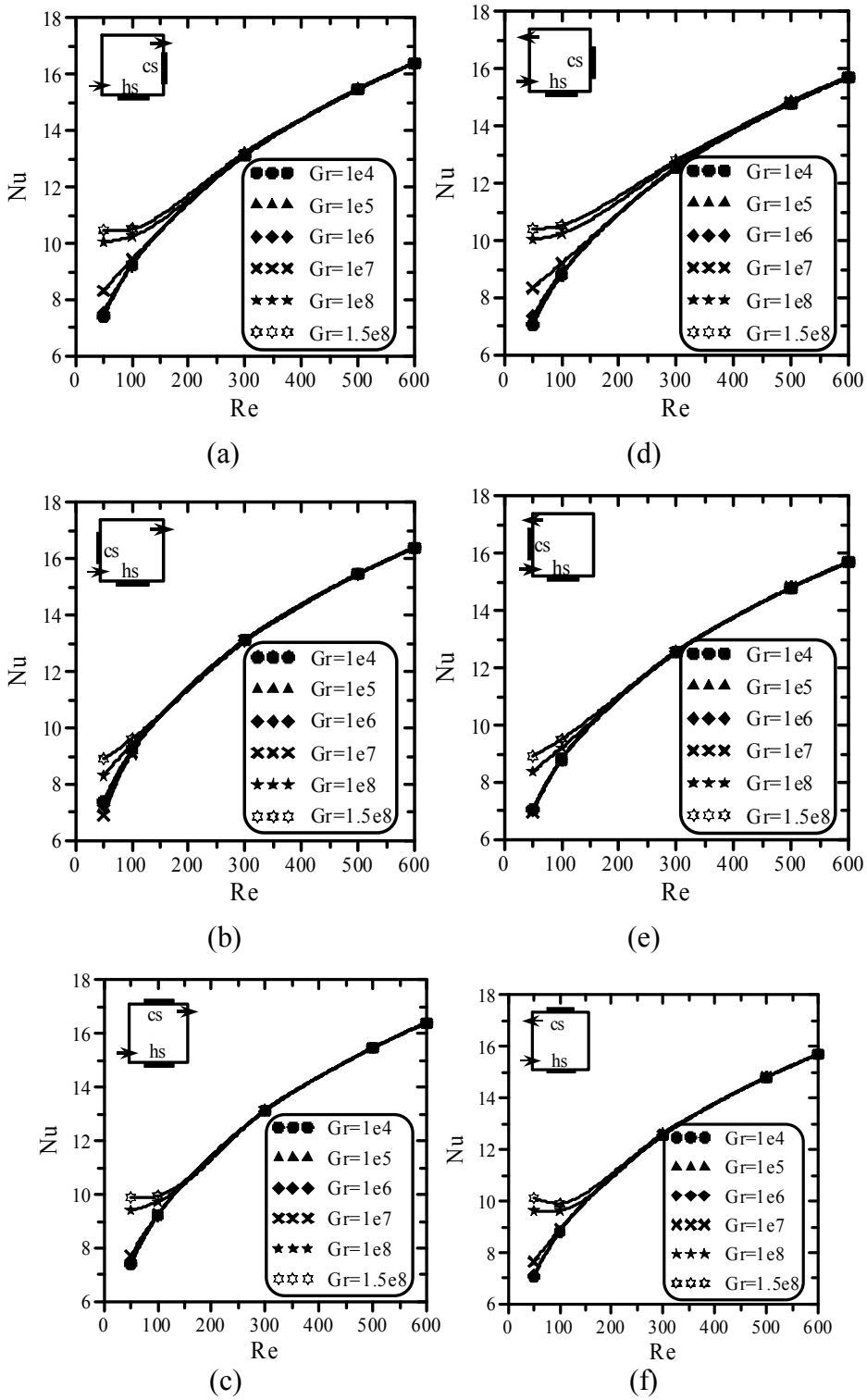

Fig. 4 Average Nusselt number for cases 1and 2

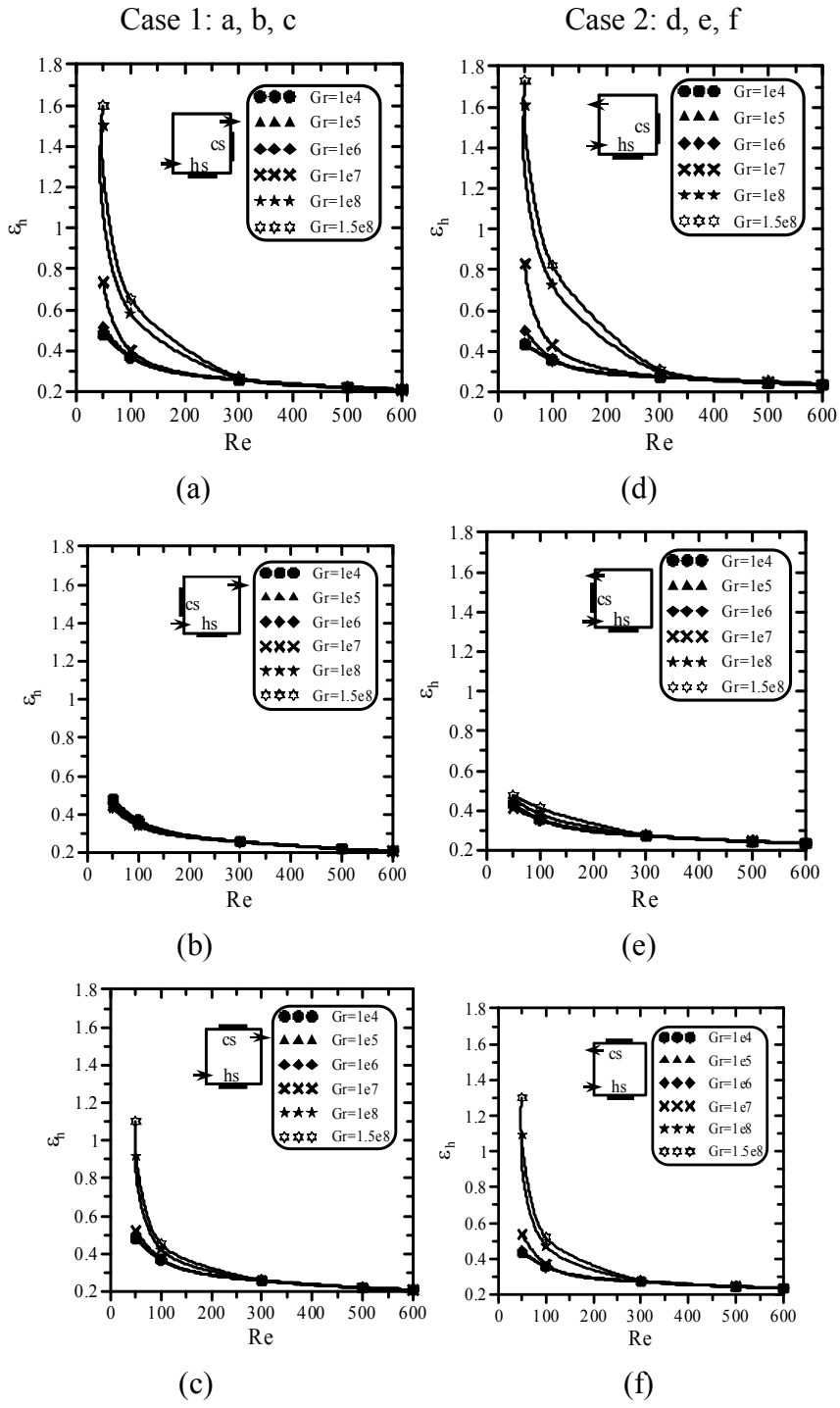

Fig. 5 Heat removal effectiveness (ε_h) for cases 1and 2
Case 1:a, b, c Case 2: d, e, f

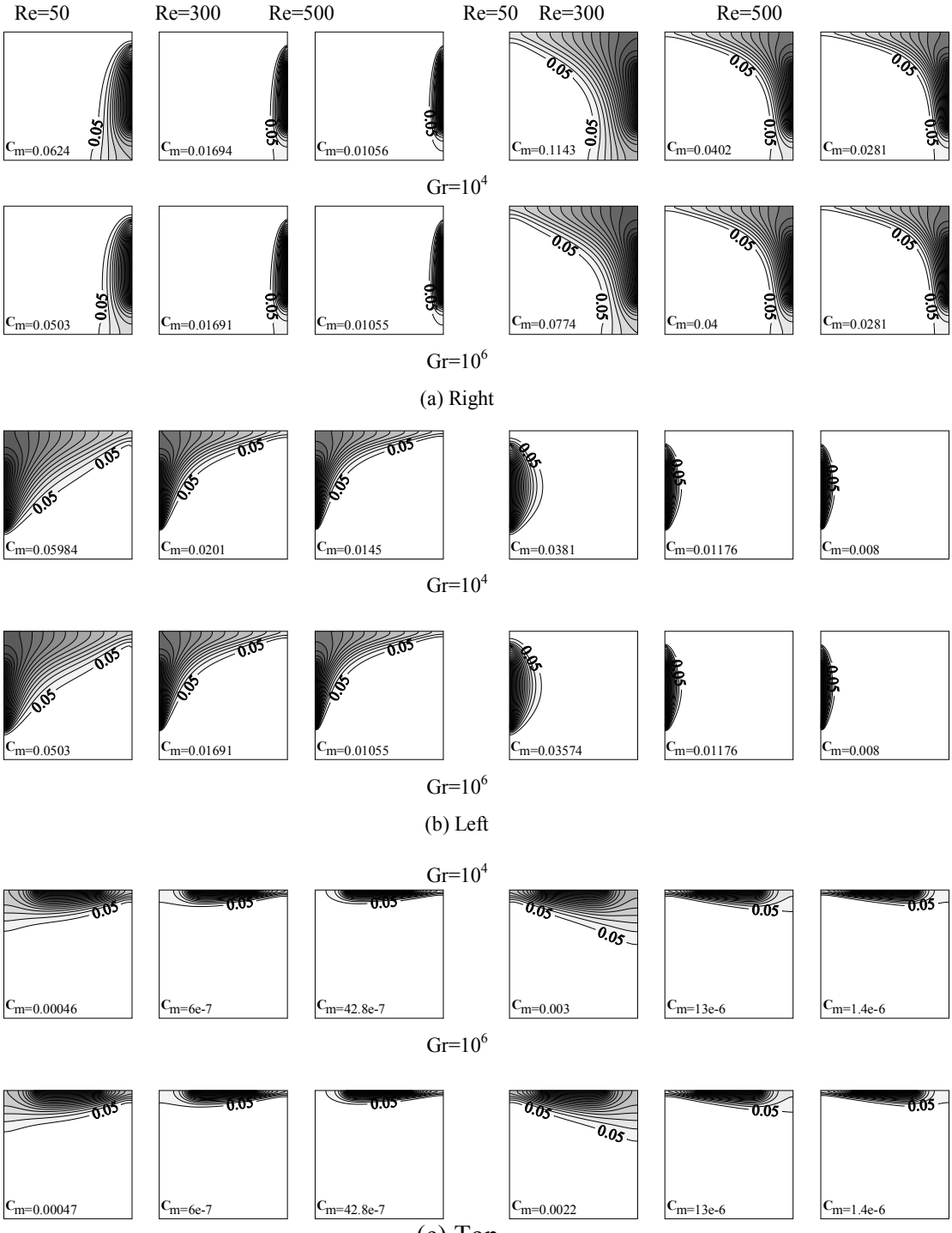

Fig. 6 Contaminant contours for different Re and Gr numbers for different locations of contaminant sources

The average Sherwood number, Sh_m, as the function of Reynolds number, Re, at different Grashof numbers for cases 1and 2 is displayed in Fig. 7. For $10^4 \langle Gr \langle 10^6$, the average Sherwood number increases with the increase of the Reynolds number due to the forced convection fully dominates the airflow structure. For $10^7 \langle Gr \leq 1.5 \times 10^8$, Sh_m decreases with the increase of Re because natural convection fully dominates the airflow structure and then increases with the increase of Re due to the natural convection gains more interaction with forced convection and therefore the transport mechanism enhanced. For $Re \rangle 300$, the average Sherwood number is little effect by increasing the Gr. At the right outlet air (case 1) and $Re = 600$, the maximum average Sherwood number was about 15.8 for the right and left contaminant sources and about 17.1 for the top contaminant source. On other hand, at the left outlet air (case 2), the maximum average Sherwood number was about 9.1, 19.7 and 16.3 for the right, left and top contaminant sources respectively at $Re = 600$.

Figure 8 shows the effect of Reynolds number on the contaminant removal effectiveness, ε_c, for different Grashof numbers. The ventilation effectiveness for contaminant removal decreases with the increasing Reynolds number for the right and left contaminant source as shown in Figs. (8a, b, d and e) while it is increases for the top contaminant source as shown in Figs. (8c, and f). For $Re \rangle 300$, the ventilation effectiveness for the right and left contaminant sources is slightly effected by increasing the Gr and Re. On the other hand, $Re \langle 300$, the ventilation effectiveness is increased by increasing the Gr and location of the outlet air due to the cooperation between the natural and forced convection is gradually enhanced. From the figure, the ventilation effectiveness in the occupied zone is higher than 1

This leads to the contaminant concentration in the occupied zone to be lower than the contaminant concentration in the outlet air. Therefore, the ventilation performance is improved in termes of air quality.

Figure 9 presents the variations of air clearing efficiency, ξ, as a function of Reynolds number, Re, at different Grashof numbers for cases 1and 2. The air clearing efficiency increases with increasing the Reynolds number. $Re \langle 300$, the air clearing efficiency is effected by increasing the Gr number due to the cooperation between the natural and forced convection is gradually enhanced. On the other hand, $Re \rangle 300$, the air clearing efficiency is nearly constant by increasing the Gr number because the forced convection dominates the airflow

structure. Increasing Reynolds number from 300 to 600 increases the air clearing efficiency with about 1.5 percent for the cases 1 and 2. This means that the locations of the contaminant source and air outlet have no major influence on the air clearing efficiency. The air clearing efficiency of the top contaminant source is globally higher than the clearing efficiency of left and right contaminant sources. The reason is that the left and right contaminant sources lie farther from the exhaust than the top source, and thus a longer transport path is required for contaminant removal, as indicated by the contamination degree. It is observed that, the quality of indoor air environment is improved.

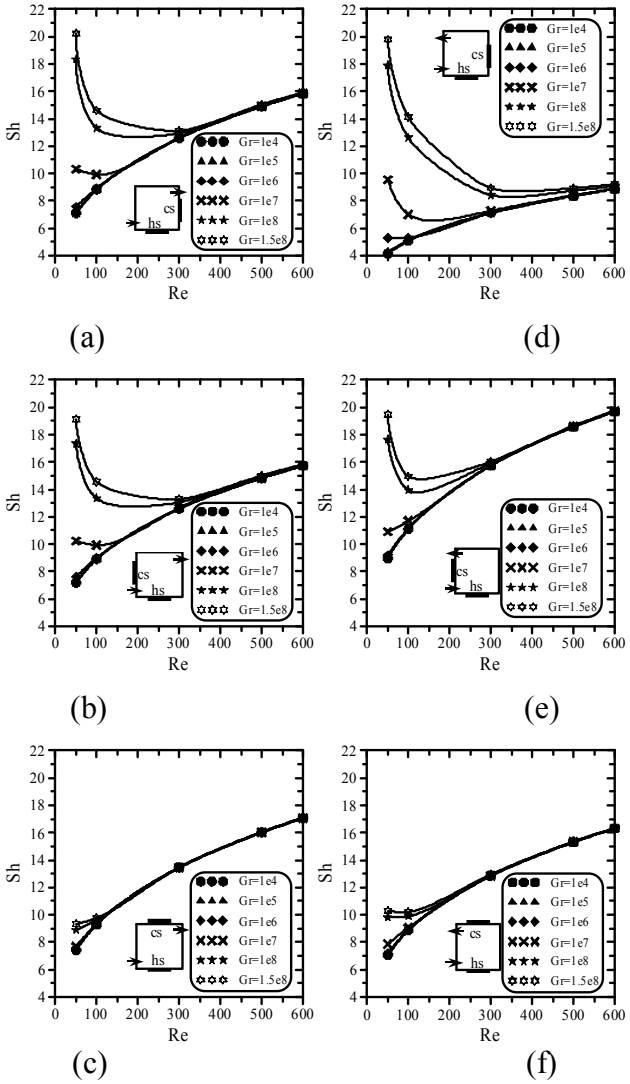

Fig. 7 Average Sherwood number for cases 1and 2
Case 1:a, b, c **Case 2: d, e, f**

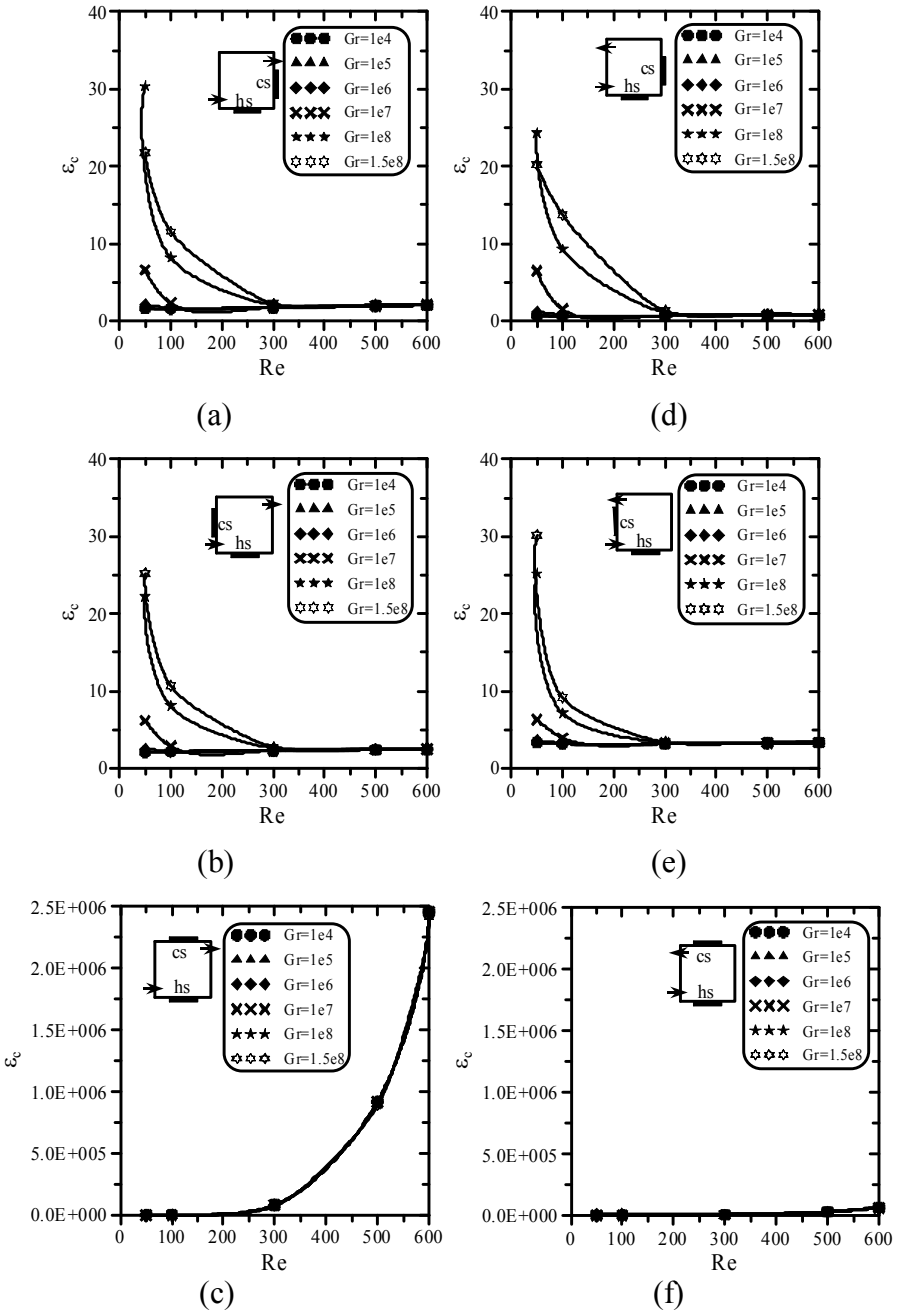

Fig. 8 Contaminant removal effectiveness (ε_c) for cases 1and 2
Case 1:a, b, c **Case 2: d, e, f**

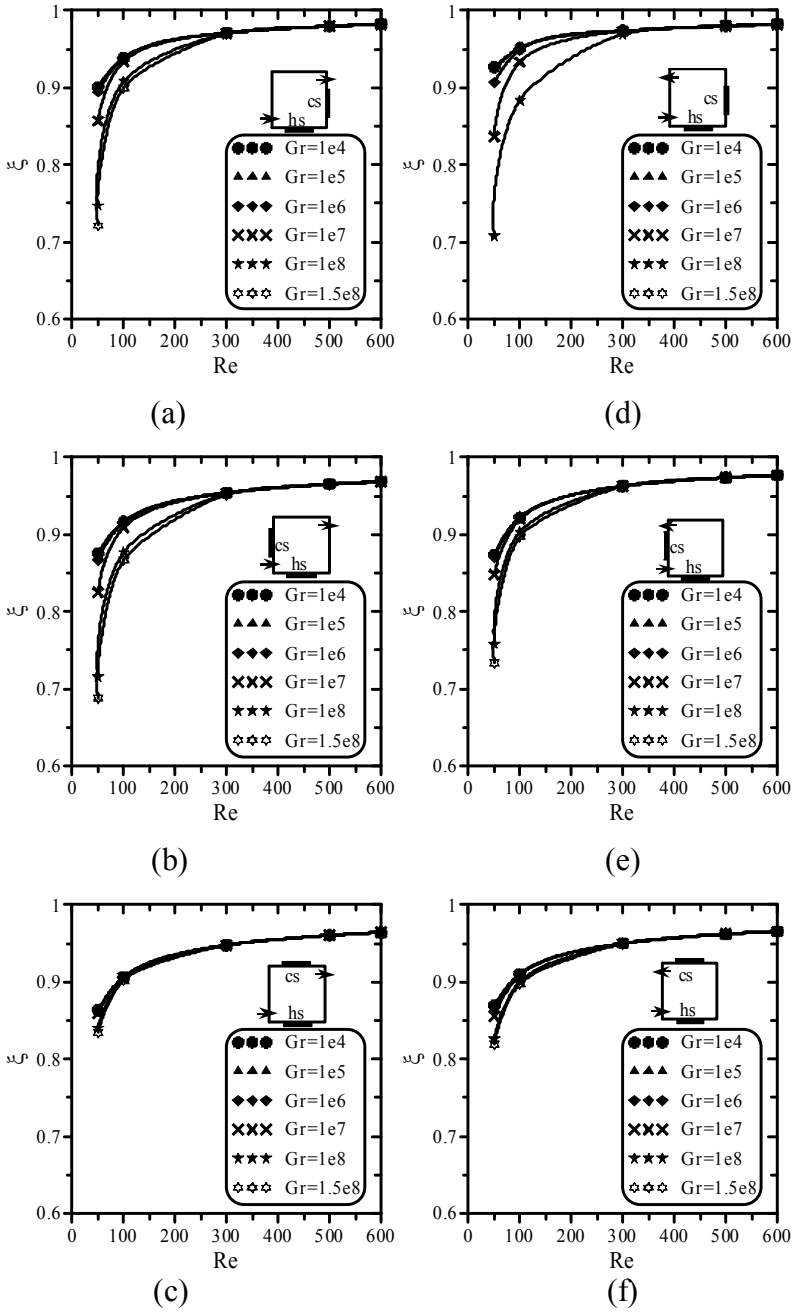

Fig. 9 Air cleaning efficiency (ξ) for cases 1and 2
Case 1:a, b, c **Case 2: d, e, f**

9 Conclusions:

Laminar steady mixed convection in a two-dimensional displacement ventilated room with discrete heat and contaminant sources is numerically investigated in the present work. The indoor air environment is determined by the interaction between the natural convection by the discrete heat and contaminant sources and the external forced convection driven by the mechanical ventilation. The discussed thermal comfort parameters include temperature distribution and ventilation effectiveness for the heat removal (ε_h). The indoor air quality is determined by investigating the contaminant distribution, ventilation effectiveness for contaminant removal (ε_c) and air cleaning efficiency (ξ). The following conclusions can be obtained:

1. The isothermal and contaminant contours provide a useful and simple means to visualize the heat and contaminant transport structures. With the increase of the Grashof and Reynolds numbers, the isothermal and contaminant contours decreases.
2. Results for different outlet locations show that the nearer the outlet is from the heat and contaminant sources, the more effective it is to vent heat and contaminant generated by the sources.
3. With the increase of Reynolds number, the heat and mass transfer rates and the air clearing efficiency increase while the heat and contaminant removal effectiveness decrease.
4. The heat and mass transfer rates, the heat and contaminant removal effectiveness and the air clearing efficiency are influenced by the locations of the contaminant source and air outlet for Reynolds number less than 300.
5. Increasing the Reynolds number more than 300, the locations of the contaminant source and air outlet have no major influence on the heat transfer rate and the heat removal effectiveness ε_h and the air clearing efficiency ξ while the mass transfer rate and the contaminant removal effectiveness is affected.
6. The air outlet is effective in contaminant removal and the location of the contaminant source is slightly in temperature removal.

References

[1] *ASHRAE, Handbook: HVAC Systems & Equipment (2000), Fundamentals (2001), Refrigeration (2002) and HVAC Applications (2003).*

[2] *B. Calcagni, F. Marsili, M. Paroncini, Natural convection heat transfer in square enclosures heated from below, Applied Thermal Engineering 25 (16) (2005) 2522–2531.*

[3] *DP. Wyon, MH. Sandberg, Thermal manikin prediction of discomfort due to displacement ventilation, ASHRAE Transactions 96 (1) (1990)*

[4] *G. Gan, Evaluation of room air distribution systems using computational fluid dynamics, Energy and Buildings 23 (1995) 83-93*

[5] *G. Gan, Numerical investigation of local discomfort in offices with displacement ventilation, Fuel and Energy 37 (2) (1996) 82–15*

[6] *H. B. Awbi, Energy efficient room air distribution, Renewable Energy 15 (1998) 293-299*

[7] *H. K Versteeg, W. Malalasekera, An introduction to computational fluid dynamics the finite volume method, John Wiley & Sons Inc., New York, 1995.*

[8] *H. Kruhne, Effect of cooled ceilings in rooms with displacement ventilation on the air quality, Proceedings of Indoor Air 93 (5) (1993) 395-400*

[9] *H. Xing, A. Hatton, H.B. Awbi, A study of the air quality in the breathing zone in a room with displacement ventilation, Building and Environment 36 (2001) 809–820*

[10] *H.-J. Park, D. Holland, The effect of location of a convective heat source on displacement ventilation: CFD study, Building and Environment 36 (2001) 883–889*

[11] *K. Fitzner, Displacement ventilation and cooled ceilings, results of laboratory tests and practical installations, Proceedings of Indoor Air'96 (1) (1996) 41-50.*

[12] *M. Behne, Indoor air quality in rooms with cooled ceilings mixing ventilation or rather displacement ventilation, Energy and Buildings 30 (1999) 155-166.*

[13] *P. V. Nielsen, Velocity distribution in a room ventilated by displacement ventilation and wall-mounted air terminal devices, Energy and Buildings 31 (2000) 179–187*

[14] *Q. Chen, P. Suter, A. Moser, Influence of air supply parameters on indoor air diffusion, Building and Environment 26 (4) (1991) 417-431*

[15] Q.-H. Deng, G.-F. Tang, Numerical visualization of mass and heat transport for mixed convective heat transfer by streamline and heatline, International Journal of Heat and Mass Transfer 45 (2002) 2387–2396.

[16] Q.-H. Deng, J. Zhou, C. Mei, Y.-M. Shen, Fluid, heat and contaminant transport structures of laminar double-diffusive mixed convection in a two-dimensional ventilated enclosure, International Journal of Heat and Mass Transfer 47 (2004) 5257–5269

[17] R. Kosonen, The effect of supply air systems on the efficiency of a ventilated ceiling, Building and Environment 42 (4) (2007) 1613-1623

[18] S. V Patankar, Numerical heat transfer and fluid flow, Hemisphere publishing company, New York, 1980

[19] Y. Zhang, X. Wang X., G.L. Riskowski, L.L. Christianson, Quantifying ventilation effectiveness for air quality control, Transactions of the American Society of Agricultural and Biological Engineers (ASABE) 44(2) (2001) 385-390.

[20] Z. Lian, Experimental study factors that affect thermal comfort in an upward-displacement air-conditioned room, HVAC and R. Research 8 (2) (2002) 191–200

[21] Z. Lin, T.T. Chow, C.F. Tsang, K.F. Fong, L.S. Chan, CFD study on effect of the air supply location on the performance of the displacement ventilation system, Building and Environment 40 (8) (2005) 1051-1067